Watching the formation and reshaping of a Fano resonance in a macroscopic medium

Yu He [0],[1] Zuoye Liu,[1,*] Nan Xue,[1] Christian Ott [0],[2] Thomas Pfeifer,[2] Adrian N. Pfeiffer,[3] and Bitao Hu[1,†]

[1]*School of Nuclear Science and Technology, Lanzhou University, 730000 Lanzhou, China*
[2]*Max-Planck-Institut für Kernphysik, Saupfercheckweg 1, 69117 Heidelberg, Germany*
[3]*Institute of Optics and Quantum Electronics, Abbe Center of Photonics, Friedrich Schiller University,*
Max-Wien-Platz 1, 07743 Jena, Germany

Time-resolved buildup of a Fano resonance in a macroscopic gaseous medium is theoretically studied by attosecond transient absorption spectroscopy. An intense near-infrared field is employed as an adjustable gate to confine the temporal dynamics, enabling one to resolve the line-shape formation in real time. Beyond the region where the single-atom approximation holds, we observe the emergence of spectral spikes with narrow linewidths for certain time delays and propagation distances, which represents that the medium can be delicately structured to be an efficient resonant absorber. Spectral substructures appear on the shoulder of the absorption lines after additional pulse propagation. The links between these features imprinted in spectral profiles and the formation of temporal characteristics in the excitation field are identified. The collective response of the medium versus time delay and propagation distance, in this laser-gated case, provides clues to the time-domain information on autoionization state and the microscopic dynamics occurring at each layer of the medium.

As attosecond science is moving from atomic physics to complex systems, the scrutiny of fundamental phenomena involving more than one electron becomes a requisite. A textbook example governed by electron-electron correlation is autoionization, where the picture of a single active electron breaks down. The resonance line shape of an autoionization state, with a characteristic asymmetric profile in the frequency domain, was explained in the seminal paper of Fano [1]. The so-called Fano profile stems from the two interfering channels from the ground state to the continuum: the direct photoionization and the resonant excitation to an unstable state followed by autoionization. Time-resolving the emergence of a Fano resonance represents an endeavor in attosecond science, which has been achieved lately in experiments based on transient absorption spectroscopy (TAS) [2,3] and photoemission spectroscopy [4]. For photoabsorption spectroscopy, an interesting situation arises when a realistic medium is considered, which requires going beyond the approximation of a thin medium and incorporating macroscopic propagation effects. Resonant pulse propagation is quite a universal phenomenon when a short pulse passes through a medium with a long-lived resonance compared with the pulse duration [5–7]. Under such a condition, the short pulse would develop a tail with temporal beats sometimes called Burnham–Chiao ringing [8]. In the past few years, resonant pulse propagation has been shown to introduce spectral modifications in the ultrafast TAS spectrum [9–12] or in the static absorption spectrum when the excitation pulse is moderately intense [13].

The efficient absorption of radiation underlies a range of applications from spectral filtering of electromagnetic waves to energy-conversion devices. By replacing the amplifying medium of the laser system with an absorbing medium, the incoming light can be perfectly captured under specific conditions. Such an optical system, related to a laser by time reversal, was referred to as a coherent perfect absorber. This concept, theoretically proposed by Chong *et al.* [14], has been experimentally realized in a silicon cavity [15] and recently in a disordered medium with an absorption of >99.78% of the injected intensity [16], which raises practical prospects in sensing, photovoltaics, and photodetection [17].

Previous investigations have qualitatively illustrated how the temporal and spectral reshaping evolves while passing through a laser-dressed two-level system [9,10] (simulations involving more states are also included therein), in which an additional pulse perturbs the polarization and facilitates the observation of propagation effects in the frequency domain. However, in this Letter, we focus on the autoionization $2s2p$ state of the helium atom, which inherently has a Fano line shape and a much shorter lifetime, and persists even in dense media such as helium nanodroplets [18]. Specifically, we monitor the formation and reshaping of the asymmetric profile in a macroscopic gaseous medium by TAS using an attosecond extreme-ultraviolet (XUV) in combination with a near-infrared (NIR) pulse. A tunable gate is created in the time domain by NIR laser-induced depletion of the XUV-excited autoionization state, allowing us to sample the ultrafast buildup of the Fano resonance. Beyond the single-atom level, sharp absorption peaks with abnormal strengths and linewidths form under appropriate conditions. The absorption could be enhanced to achieve a nearly complete extinction of incoming light at resonance energy. As the medium becomes denser, the absorption spectrum undergoes further modifications, and spectral substructures near the line center are observed. The relations of these phenomena with

---

*Corresponding author: zyl@lzu.edu.cn
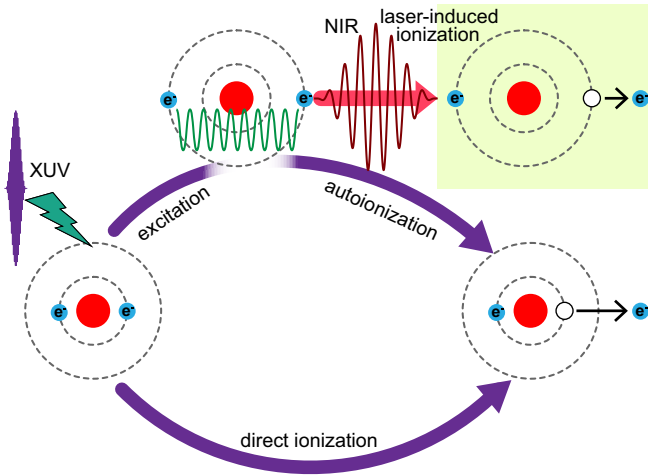†Corresponding author: hubt@lzu.edu.cn

FIG. 1. The direct and indirect (purple curved arrows) ionization of helium irradiated by an extreme-ultraviolet (XUV) laser field. The interference of the two quantum paths gives rise to the Fano profile in the frequency domain. Since the autoionization occurs on a timescale of tens of femtoseconds, the indirect path can be effectively turned off with an auxiliary pulse by laser-induced ionization (red horizontal arrow). Turning the interval between the excitation and ionization allows us to resolve the buildup of the Fano resonance.

the XUV temporally emerged signatures are identified. The collective response of the system contains temporally and spatially resolved dynamics, yielding insights into ultrafast autoionization dynamics with a propagation-shaped excitation pulse and the possibility of manipulating Fano interferences in dense media with strong laser fields.

The process of interest is shown in Fig. 1; with helium atoms being the target sample, it is conceptually similar to the scheme recently demonstrated in Ref. [2]. The atomic system we consider consists of a ground state $1s^2$ and a doubly excited state $2s2p$ embedded in a background continuum $1sEp$, which is exposed to a 500 as full width at half maximum (FWHM) duration single attosecond pulse with a peak intensity of 10^{11} W/cm^2. The 60.15 eV central photon energy is resonant to the $1s^2$-$2s2p$ transition. The NIR pulse has a central wavelength of 760 nm, an FWHM duration of 7 fs, a peak intensity of 20 TW/cm^2, and is delayed by τ with respect to the XUV pulse centered at $t = 0$. Both pulses have initial Gaussian profiles in the time domain. To illustrate the expected line-shape formation and reshaping during resonant pulse propagation, the total wave equation is expanded as $|\Psi(t, \tau)\rangle = c_g(t, \tau)|1s^2\rangle + e^{-i\omega_X t}[c_b(t, \tau)|2s2p\rangle + \int c_E(t, \tau)|1sEp\rangle dE]$, where ω_X is the central frequency of the XUV pulse. Adopting the adiabatic elimination of the continuum and the rotating wave approximation for the XUV coupling for its high frequency and low intensity (peak Rabi frequency of 1.7 meV) [19], the associated coefficients and hence the dipole response in the presence of the XUV pulse only can be obtained by solving the time-dependent Schrödinger equation. In the simulation, the dipole matrix element between $1s^2$ and $2s2p$, the autoionization decay time, and the Fano asymmetry parameter are 0.038 a.u. [20], 17 fs, and -2.77 [21], respectively. The action of the NIR field ionization is analytically incorporated through an ionization rate $\Gamma_4(t, \tau) = \alpha_4 I_{\text{NIR}}^4(t, \tau)$, i.e.,

$\langle 2s2p|H(t, \tau)|2s2p\rangle = E_b - i\Gamma_4(t, \tau)$, with $H(t, \tau)$ being the time- and delay-dependent Hamiltonian and E_b the field-free energy of $2s2p$ state. The power of 4 denotes the number of NIR photons (1.63 eV central photon energy) required to reach the $N = 2$ ionization threshold of 65.40 eV, leaving the residual helium ion in an excited state, since the Keldysh parameter [22] $\gamma > 1$ for the used NIR intensity. Here, α_4 is chosen to achieve comparable depletion of the $2s2p$ state on time delay and NIR intensity with the *ab initio* calculation in Ref. [2]. The XUV pulse area is relatively small, and the depletion of the ground state is negligible; thus, the contribution of electrons freed by autoionization, XUV direct ionization, and NIR ionization to the refractive index is safely ignored. For a loosely focused laser beam, calculations with the frequency-domain three-dimensional propagation equation [23] and the one-dimensional (1D) equation [24] were confirmed to yield similar results. Therefore, it is sufficient and more convenient to employ the 1D one, which was formulated in a reference frame moving with the laser pulses at the speed of light in vacuum, to keep track of the XUV field as it travels through the target. The absorption spectrum is characterized by optical density (OD) defined as $\text{OD}(\omega, \tau) = -\log_{10}[I(\omega, \tau)/I_0(\omega)]$, where $I(\omega, \tau)$ and $I_0(\omega)$ are XUV spectra at the exit and the entrance of the medium, respectively. For a given system, propagation effects are determined by the pathlength-density product. A 2-mm-long helium medium is considered hereafter unless otherwise specified, and the atomic number density (target pressure) is changed in the simulations. In this model, the three states specified above are our focus, and the actual wavelength of the ionization laser is less important. The excitation and coupling of other resonances would complicate both the XUV spectral and temporal profiles [25], making the encoded information less extractable. However, the general mechanism we are concerned with still remains, and the additional processes are thus disregarded in the simulations; a similar treatment has been successfully applied before at the single-atom level [2], which is capable of reproducing the measured characteristics.

The calculated transient-absorption spectra for three different atomic densities are plotted in Fig. 2. We are interested in positive time delays at which the XUV excitation and NIR ionization occur in sequential order. Starting the computations at several femtoseconds before time zero is sufficient to cover most of the XUV pulse of 0.5 fs FWHM duration and, hence, the dynamics of interest. For the low-density case shown in Fig. 2(a), the spectral evolution can be understood intuitively. The dynamic buildup of the Fano resonance is triggered by the excitation XUV pulse. Shortly after the two pulses overlap, the resonance line shape is smeared out as little time is left for the polarization to oscillate freely. The natural relaxation pathway is severely interrupted, and the indirect path to the continuum dominates, modifying the consequence of the interference. By increasing the time delay between the two pulses, the confining gate becomes wider, and more information about the doubly excited resonance survives. The absorption line becomes narrower and clearer, and the original Fano profile gradually builds up. The atomic density in Fig. 2(a) is low enough that the absorbance of the medium typically resembles the single-atom optical density $\text{OD}_s(\omega, \tau) \propto -\omega\text{Im}[\tilde{d}(\omega, \tau)/\tilde{E}(\omega)]$ [24], with $\tilde{d}(\omega, \tau)$ denoting the dipole
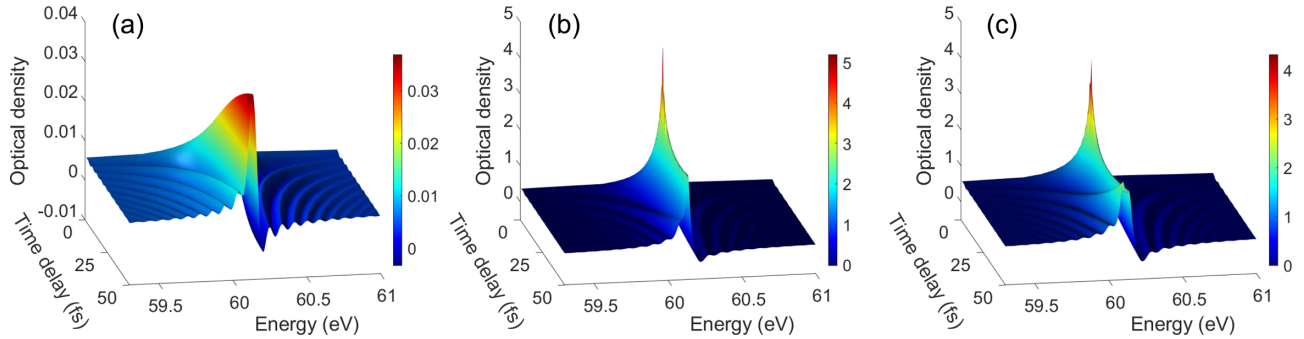
FIG. 2. Transient absorption spectra in the vicinity of the $2s2p$ resonance energy for different atomic densities. For a relatively low density of (a) 4.0×10^{16} cm^{-3}, the spectrum closely resembles what is actually measured in Ref. [2]. By contrast, for denser media with atomic densities of (b) 2.6×10^{18} and (c) 4.0×10^{18} cm^{-3}, the spectra are completely reshaped with spikes and additional spectral features.

response and $\tilde{E}(\omega)$ the XUV pulse spectrum. For a higher atomic density in Fig. 2(b), the entire profile changes drastically and deviates from the low-density behavior. A narrow, sharp peak emerges near the line center, which is much higher than the absorption peak shown at longer time delays. As OD is defined as the decadic logarithm of the intensity ratio here, OD values exceeding 4 indicate that $>99.99\%$ of the incident XUV intensity at resonance energy is absorbed. In this case, the system absorbs the resonance frequency of the injected light almost completely with a narrow linewidth, which may be regarded as an efficient resonant absorber. An even higher atomic density witnesses further modifications, as shown in Fig. 2(c). The spectral spike moves to smaller time delays, and a spectral substructure, shown as the second peak on the shoulder of the absorption line at smaller photon energies, is emerging and even dominating at longer time delays.

To address how the XUV pulse is spectrally reshaped with the formation of novel features during resonant pulse propagation and the connection with its temporal structure, in Figs. 3(b) and 3(d), we compute the macroscopic line shapes for a set of medium layers at 20 and 40 fs time delays, respectively, with a density of 4.0×10^{18} cm^{-3} (about 160 mbar gas pressure at room temperature). The corresponding evolutions of the single-atom optical density OD$_s$ with medium position are shown in Figs. 3(a) and 3(c) to assist analysis, and the associated electric field envelopes are plotted in Fig. 3(e). As discussed before, the temporal structure of the excitation pulse gets prolonged during propagation owing to the interplay between the induced polarization and the original field. Thus, the absorption spectra in Figs. 3(a) and 3(c) represent the microscopic single-atom responses stimulated with propagation-shaped XUV fields. However, we would like to emphasize that the ionization-gated case is qualitatively different from the previous investigation in which the effect of NIR is modeled as a time-dependent phase accumulating on the upper state amplitude [10]. Here, the trailing end of the XUV barely extends outside the gate as its stimulating polarization is terminated by the NIR pulse. Nevertheless, a series of subpulses can still develop within the gate as the pulse travels further, albeit only two subpulses at most are exhibited for the parameters used in Fig. 3(e). Initially, the macroscopic absorption profile builds up steadily with increasing propagation distance for either 20 or 40 fs time delays in Figs. 3(b) and 3(d), respectively. Afterwards, the absorbance reaches a

maximum before seeing a decrease at a relatively large propagation distance. Around the position where the transition takes place, the single-atom results at resonance energy switch remarkably from absorption to emission. Moreover, the enclosed area of the first subpulse there becomes comparable with that of the main pulse, which denotes a delicate balance between the out-of-phase polarizations and accounts for the nonlinear spectral evolution. This connection can be mathematically explained as follows: in the present case that the central frequency of the XUV pulse ω_X and the transition frequency ω_0 share the same value, the XUV electric field after propagation through a certain distance can be expressed as

$$E(t, x) = F(t, x)e^{i\omega_0 t} + \text{c.c.} = [F_m(t, x) + F_s(t, x)]e^{i\omega_0 t} + \text{c.c.},$$

$$(1)$$

where $F(t, x)$ denotes the field envelope of the whole pulse, $F_m(t, x)$ and $F_s(t, x)$ the field envelopes of the main pulse and the subpulses, respectively. After Fourier transformation, the positive-frequency electric field is given by

$$\tilde{E}(\omega, x) = \frac{1}{\sqrt{2\pi}} \int_{-\infty}^{\infty} F(t, x)e^{i(\omega_0 - \omega)t}dt$$

$$= \frac{1}{\sqrt{2\pi}} \int_{-\infty}^{\infty} [F_m(t, x) + F_s(t, x)]e^{i(\omega_0 - \omega)t}dt. \quad (2)$$

The described sharp absorption peak would in principle emerge when the modulus of $\tilde{E}(\omega, x)$ drops to zero or a very small amount during propagation. Owing to the asymmetric characteristic of the Fano resonance, the position of the absorption peak is not centered at the resonant frequency. As a result, the observation of the efficient absorption is exhibited at a frequency ω slightly detuned from ω_0 and at the spatial position where $|\tilde{E}(\omega, x)| \approx 0$ holds. As a consequence, the area enclosed by the main-pulse envelope and that by the envelope of the subpulses (here just referring to the first subpulse from our calculation) are only approximately equal in this case. A wider temporal gate (longer NIR delay) accelerates the balance, and the enhanced resonant absorption behavior would exhibit at a shorter propagation distance [cf. Figs. 3(b) and 3(d)]. A higher atomic density has a similar effect, and a shorter temporal gate is correspondingly required for the excitation field to develop the balance [cf. Figs. 2(b) and 2(c)].
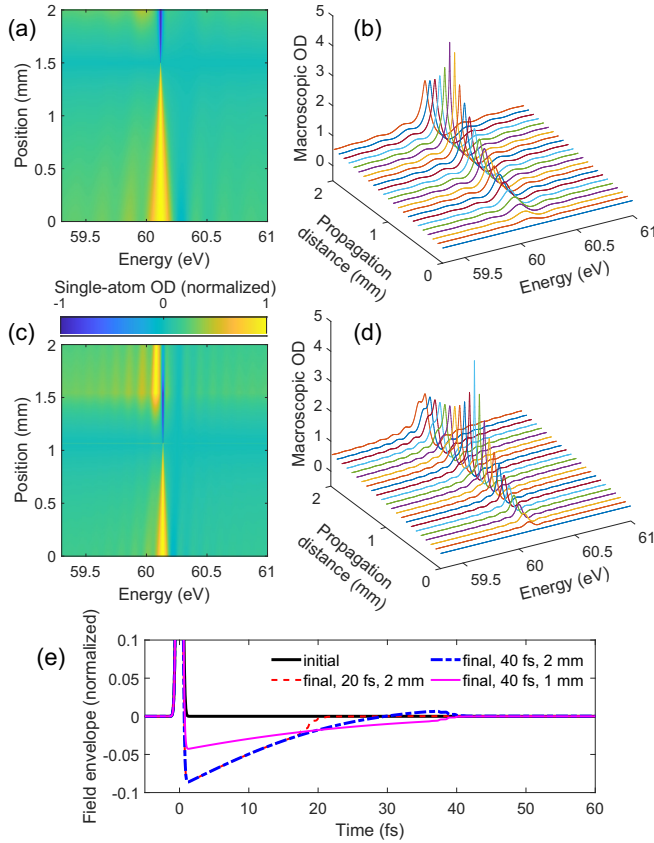
FIG. 3. Sliced simulations of the single-atom and macroscopic transient absorption. Single-atom absorption spectra along the propagation direction with an atomic density of 4.0×10^{18} cm^{-3} for (a) 20 and (c) 40 fs time delays. Their corresponding buildup of macroscopic profiles for a series of propagation distances is shown in (b) and (d), respectively. To enable comparison, the single-atom line shapes are depicted in units of OD$_s$ normalized to the maximum absolute value at each layer. (e) Real parts of the extreme-ultraviolet (XUV) field envelopes (normalized to unity) at the beginning of the medium and at propagation distances of 1 and 2 mm for 20 and 40 fs time delays, respectively. A trailing tail consisting of subpulses is developed within the gate.

However, it is noteworthy that the sharpening of the resonance in the frequency domain does not imply an extended XUV time scale, which is somewhat counterintuitive at first glance, but rather results from the computation of the optical density. Figure 4 shows the OD profile at around the optimal absorption position in Fig. 3(b) together with the associated laser spectra and temporal envelopes. A dip reaching very close to zero is clearly exhibited in the transmitted spectrum shown in Fig. 4(b), but its corresponding time profile of the electric field envelope is still confined within the gate, as shown in Fig. 4(c). The absorption spectrum with respect to medium length supplies information on microscopic processes that happen at each layer, as it records the collective response of the system and represents approximately an average over the single-atom results with propagation distance. The appearance of the second subpulse at a longer time delay after additional propagation [cf. the magenta and dash-dotted blue lines in Fig. 3(e)] is consistent with the macroscopic
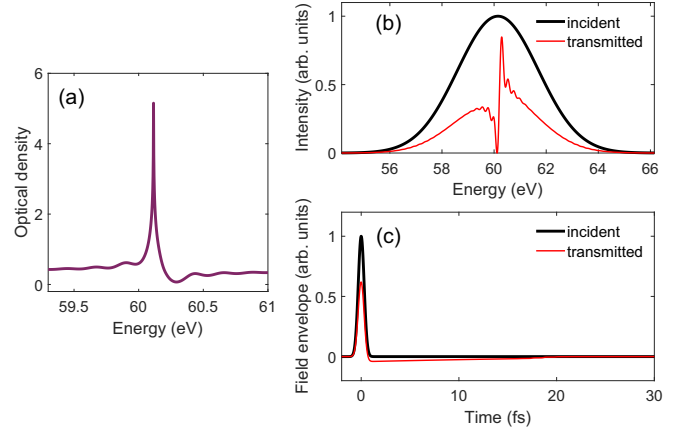

FIG. 4. (a) The (macroscopic) optical density of the system after propagating through the gas with a distance of 1.5 mm and an atomic density of 4.0×10^{18} cm^{-3} for 20 fs time delay, which roughly corresponds to the optimal absorption position in Fig. 3(b). The corresponding transmitted spectrum and field envelope together with the initial ones, are shown in (b) and (c), respectively.

OD spectrum shown in Fig. 3(d) where a newly developed absorption peak near the line center becomes visible. This spectral substructure can be understood as the consequence of the interference between the second subpulse, bearing an electric field out of phase with that of the first subpulse, and the other part of the XUV pulse. Whereas in Fig. 3(b), the gate effectively closes at around 20 fs ahead of the buildup of the second subpulse [cf. the dash-dotted blue and dashed red lines in Fig. 3(e)], and accordingly, no subfeature in the OD spectra manifests. Consequently, the reshaped temporal profile reflects spectral fingerprints and vice versa, which are generally in accordance with the conclusions drawn before [10,25]. Additionally, we wish to note that the characteristic nature that the Fano resonance is asymmetric, corresponding to a phase shift created by configuration interaction associated with electron-electron interaction [26], is intimately connected to the emergence of the spectral substructures. Such observations do not appear in the same simulation (not shown) with an identical $2s2p$ decay rate but for the absence of the background continuum $1sEp$, which is equivalent to the case of an ionization-gated Lorentzian resonance.

In summary, the ionization-gated buildup and reshaping of a Fano resonance in a dense gaseous medium has been explored during resonant pulse propagation. Novel signatures in absorption lines are connected with the temporal characteristics of the excitation XUV field: the efficient resonant absorption peak emerges when the areas of the main pulse and the first subpulse become comparable; the appearance of the second subpulse signals the emergence of the double-peaked line-shape structure. The concerted absorption over a certain distance may be harnessed to trigger interesting avenues for optical switches, filters, or other future applications. The single-atom prediction differs from the collective response of the system and hence does not represent what will actually be measured in a rather dense gaseous medium. Our results also suggest that the absorbance of the system could be switched very drastically through the delay of NIR pulse and optical

depth, which marks possibilities of controlling attosecond dynamics.

[1] U. Fano, Effects of configuration interaction on intensities and phase shifts, Phys. Rev. **124**, 1866 (1961).

[2] A. Kaldun, A. Blättermann, V. Stooß, S. Donsa, H. Wei, R. Pazourek, S. Nagele, C. Ott, C. D. Lin, J. Burgdörfer, and T. Pfeifer, Observing the ultrafast buildup of a fano resonance in the time domain, Science **354**, 738 (2016).

[3] V. Stooß, P. Birk, A. Blättermann, M. Hartmann, G. D. Borisova, C. Ott, and T. Pfeifer, Strong-field-gated buildup of a Rydberg series, Phys. Rev. Research **2**, 032041(R) (2020).

[4] V. Gruson, L. Barreau, Á. Jiménez-Galan, F. Risoud, J. Caillat, A. Maquet, B. Carré, F. Lepetit, J.-F. Hergott, T. Ruchon, L. Argenti, R. Taïeb, F. Martín, and P. Salières, Attosecond dynamics through a fano resonance: Monitoring the birth of a photoelectron, Science **354**, 734 (2016).

[5] M. D. Crisp, Propagation of small-area pulses of coherent light through a resonant medium, Phys. Rev. A **1**, 1604 (1970).

[6] G. L. Lamb, Analytical descriptions of ultrashort optical pulse propagation in a resonant medium, Rev. Mod. Phys. **43**, 99 (1971).

[7] U. Van Bürck, Coherent pulse propagation through resonant media, Hyperfine Interact. **123**, 483 (1999).

[8] D. C. Burnham and R. Y. Chiao, Coherent resonance fluorescence excited by short light pulses, Phys. Rev. **188**, 667 (1969).

[9] A. N. Pfeiffer, M. J. Bell, A. R. Beck, H. Mashiko, D. M. Neumark, and S. R. Leone, Alternating absorption features during attosecond-pulse propagation in a laser-controlled gaseous medium, Phys. Rev. A **88**, 051402(R) (2013).

[10] C.-T. Liao, A. Sandhu, S. Camp, K. J. Schafer, and M. B. Gaarde, Beyond the Single-Atom Response in Absorption Line Shapes: Probing a Dense, Laser-Dressed Helium Gas with Attosecond Pulse Trains, Phys. Rev. Lett. **114**, 143002 (2015).

[11] C.-T. Liao, A. Sandhu, S. Camp, K. J. Schafer, and M. B. Gaarde, Attosecond transient absorption in dense gases: Exploring the interplay between resonant pulse propagation and laser-induced line-shape control, Phys. Rev. A **93**, 033405 (2016).

[12] Y. He, R. Chen, F. Wang, A. N. Pfeiffer, Y. Zhang, Z. Cui, J. Ding, Z. Liu, and B. Hu, Macroscopic transient absorption in a v-type three-level system, J. Phys. B: At., Mol. Opt. Phys. **53**, 175601 (2020).

[13] Y. He, Z. Liu, Z. Cui, Y. Zhang, A. N. Pfeiffer, T. Pfeifer, J. Ding, and B. Hu, Signatures of self-modulation effects during pulse propagation in single-pulse absorption spectra, Phys. Rev. A **99**, 053418 (2019).

[14] Y. D. Chong, L. Ge, H. Cao, and A. D. Stone, Coherent Perfect Absorbers: Time-Reversed Lasers, Phys. Rev. Lett. **105**, 053901 (2010).

[15] W. Wan, Y. Chong, L. Ge, H. Noh, A. D. Stone, and H. Cao, Time-reversed lasing and interferometric control of absorption, Science **331**, 889 (2011).

[16] K. Pichler, M. Kühmayer, J. Böhm, A. Brandstötter, P. Ambichl, U. Kuhl, and S. Rotter, Random anti-lasing through coherent perfect absorption in a disordered medium, Nature **567**, 351 (2019).

[17] D. G. Baranov, A. Krasnok, T. Shegai, A. Alù, and Y. Chong, Coherent perfect absorbers: Linear control of light with light, Nat. Rev. Mater. **2**, 17064 (2017).

[18] A. C. LaForge, D. Regina, G. Jabbari, K. Gokhberg, N. V. Kryzhevoi, S. R. Krishnan, M. Hess, P. O'Keeffe, A. Ciavardini, K. C. Prince, R. Richter, F. Stienkemeier, L. S. Cederbaum, T. Pfeifer, R. Moshammer, and M. Mudrich, Fano resonances observed in helium nanodroplets, Phys. Rev. A **93**, 050502(R) (2016).

[19] W.-C. Chu and C. D. Lin, Absorption and emission of single attosecond light pulses in an autoionizing gaseous medium dressed by a time-delayed control field, Phys. Rev. A **87**, 013415 (2013).

[20] W.-C. Chu and C. D. Lin, Photoabsorption of attosecond XUV light pulses by two strongly laser-coupled autoionizing states, Phys. Rev. A **85**, 013409 (2012).

[21] C. Ott *et al.*, Strong-Field Extreme-Ultraviolet Dressing of Atomic Double Excitation, Phys. Rev. Lett. **123**, 163201 (2019).

[22] L. Keldysh, Ionization in the field of a strong electromagnetic wave, Sov. Phys. JETP **20**, 1307 (1965).

[23] M. B. Gaarde, C. Buth, J. L. Tate, and K. J. Schafer, Transient absorption and reshaping of ultrafast XUV light by laser-dressed helium, Phys. Rev. A **83**, 013419 (2011).

[24] R. Santra, V. S. Yakovlev, T. Pfeifer, and Z.-H. Loh, Theory of attosecond transient absorption spectroscopy of strong-field-generated ions, Phys. Rev. A **83**, 033405 (2011).

[25] M. Wu, S. Chen, S. Camp, K. J. Schafer, and M. B. Gaarde, Theory of strong-field attosecond transient absorption, J. Phys. B: At., Mol. Opt. Phys. **49**, 062003 (2016).

[26] C. Ott, A. Kaldun, P. Raith, K. Meyer, M. Laux, J. Evers, C. H. Keitel, C. H. Greene, and T. Pfeifer, Lorentz meets Fano in spectral line shapes: A universal phase and its laser control, Science **340**, 716 (2013).

Correction: The previously published Figure 3(e) contained a plotting error in the dashed red line and has been replaced.